Development 125, 2087-2098 (1998)
Printed in Great Britain © The Company of Biologists Limited 1998
DEV6324

sma-1 encodes a β_H-spectrin homolog required for *Caenorhabditis elegans* morphogenesis

Caroline McKeown*, Vida Praitis* and Judith Austin†

Department of Molecular Genetics and Cell Biology, University of Chicago, Chicago, IL 60637, USA
*Both authors contributed equally to this work
†Author for correspondence

Accepted 20 March; published on WWW 6 May 1998

SUMMARY

Morphogenesis transforms the *C. elegans* embryo from a ball of cells into a vermiform larva. During this transformation, the embryo increases fourfold in length; present data indicates this elongation results from contraction of the epidermal actin cytoskeleton. In *sma-1* mutants, the extent of embryonic elongation is decreased and the resulting *sma-1* larvae, although viable, are shorter than normal. We find that *sma-1* mutants elongate for the same length of time as wild-type embryos, but at a decreased rate. The *sma-1* mutants we have isolated vary in phenotypic severity, with the most severe alleles showing the greatest decrease in elongation rate. The *sma-1* gene encodes a homolog of β_H-spectrin, a novel β-spectrin isoform first identified in *Drosophila*. *sma-1* RNA is expressed in epithelial tissues in the *C. elegans* embryo: in the embryonic epidermis at the start of morphogenesis and subsequently in the developing pharynx, intestine and excretory cell. In *Drosophila*, β_H-spectrin associates with the apical plasma membrane of epithelial cells; β-spectrin is found at the lateral membrane. We propose that SMA-1 is a component of an apical membrane skeleton in the *C. elegans* embryonic epidermis that determines the rate of elongation during morphogenesis.

Key words: *C. elegans*, Morphogenesis, Actin cytoskeleton, Spectrin

INTRODUCTION

Morphogenesis, the creation of form during development, occurs by a diverse set of mechanisms including cell proliferation, cell migration and changes in cell shape. Coordination of morphogenetic changes in individual cells can create large-scale changes at the level of the tissue or whole organism. A striking example of this is seen in *C. elegans* where, during morphogenesis, cell elongation produces a fourfold increase in the length of the embryo (Sulston et al., 1983; Priess and Hirsh, 1986).

Previous work suggested that the outermost cell layer, the epidermis, has a critical role in altering the shape of the embryo during *C. elegans* morphogenesis (Priess and Hirsh, 1986). The cells of the epidermis originate on the dorsal surface of the embryo and migrate ventrally to enclose the embryo at the start of morphogenesis (Priess and Hirsh, 1986; Williams-Masson et al., 1997). Shortly after the epidermis encloses the embryo, the epidermal actin cytoskeleton reorganizes, forming an array of parallel actin fibers, and the embryo begins to elongate (Priess and Hirsh, 1986). These actin fibers are located just under the apical plasma membrane of the epidermis, oriented around the circumference of the embryo and perpendicular to its anterior-posterior axis. As elongation progresses, the actin fibers decrease in length and there is a corresponding decrease in width and increase in length of the epidermal cells. Embryonic elongation is dependent on the actin cytoskeleton: treatment with cytochalasin D prevents elongation and causes elongating embryos to retract to almost their original length (Priess and Hirsh, 1986). Based on these observations, it is believed that contraction of the epidermal actin fibers generates the force that causes the change in epidermal cell shape and constricts the underlying cell layers, resulting in elongation of the embryo.

Subsequent studies have lent support to the proposed role of the epidermal actin cytoskeleton in *C. elegans* morphogenesis. Recent work has shown that the *hmp-1*, *hmp-2* and *hmr-1* genes encode *C. elegans* homologs of α-catenin, β-catenin and cadherin, respectively, and that all three are required to anchor the circumferential actin fibers to the epidermal adherens junctions (Costa et al., 1998). *hmp-1* and *hmp-2* mutant embryos begin elongation, but then retract back to their original length as the actin fibers in the dorsal epidermis detach from the adherens junctions. In *hmr-1* mutants, detachment of epidermal actin fibers is also observed, although defects in epidermal enclosure of the embryo prevent elongation. In these mutants, the actin fibers continue to decrease in length after separation from the adherens junctions, supporting the model that during morphogenesis they provide the contractile force required for elongation of the *C. elegans* embryo. Although there is no direct evidence for the presence of myosin in the epidermal actin fibers, mutations in *let-502*, a *C. elegans*

member of the family of Rho kinases, block normal elongation; this phenotype is suppressed by mutations in the *mel-11* gene, which encodes a homolog of the regulatory subunit of smooth muscle myosin phosphatase (Wissman et al., 1997). Together, these results point to a central role for the epidermal actin cytoskeleton in *C. elegans* morphogenesis.

In this paper, we describe experiments which show that the *sma-1* gene is required for a normal rate of elongation during embryonic morphogenesis. We find that *sma-1* embryos are viable but elongate slowly, resulting in abnormally short larvae. Morphogenesis of the pharynx and the excretory cell are also abnormal. *sma-1* RNA is expressed in the epidermis during early morphogenesis, suggesting that SMA-1 acts in the epidermis during elongation. In addition, the presence of *sma-1* RNA in the developing pharynx and excretory cell points to an independent role for SMA-1 in the morphogenesis of these tissues.

sma-1 encodes a homolog of β_H-spectrin, a novel spectrin isoform identified as the product of the *Drosophila Karst* gene (Dubreuil et al., 1990; Thomas et al., 1998). Spectrin is a heterodimeric actin-binding protein, composed of α- and β-spectrin subunits, that forms a cytoskeletal network associated with the plasma membrane (Bennett and Gilligan, 1993). β_H-spectrin contains additional spectrin repeats and an SH3 domain not present in conventional β-spectrins, and shows non-conservation of an ankyrin-binding sequence present in β-spectrin (Dubreuil et al., 1990; Thomas et al., 1997). In the cell, β- and β_H-spectrins form non-overlapping regions of membrane skeleton; in epithelial cells, β-spectrin is associated with the lateral plasma membrane and β_H-spectrin is found in the apical region of the cell (de Cuevas et al., 1996; Lee et al., 1997; Dubreuil et al., 1997). As described in the accompanying paper (Thomas et al., 1998), *Karst* mutants have defects in eye development that indicate that β_H-spectrin is required for appropriate signaling between developing ommatidia. Based on the *sma-1* mutant phenotype and similarity between SMA-1 and β_H-spectrin, we propose that SMA-1 plays both structural and regulatory roles during morphogenesis of the *C. elegans* embryo.

MATERIALS AND METHODS

General methods and strains

Maintenance of worm strains was as described by Brenner (1974). All strains were grown at 20°C. The wild-type parent of all strains used was *C. elegans* var. Bristol, strain N2. In addition to the *sma-1* alleles described below, the following mutations were used: *fem-1(hc17ts)* IV, *unc-42(e270)*V, *daf-11(m84)*V, *sma-1(e30)V* (Hodgkin, 1997). *sma-1* mutants used in all experiments were self-progeny of homozygous *sma-1* hermaphrodites. Living animals were observed using Nomarski differential interference contrast microscopy.

Isolation of *sma-1* alleles

Three EMS-induced mutations (*mu81*, *mu82* and *mu83*), isolated in an F_1 clonal screen, were shown to be *sma-1* alleles based on phenotype, map position and failure to complement *sma-1(e30)*. We obtained seven additional EMS-induced *sma-1* alleles (*ru1, ru2, ru3, ru9, ru10, ru11* and *ru12*) and nine psoralen-induced alleles (*ru6, ru7, ru13, ru14, ru15, ru16, ru17, ru18* and *ru19*) using a *sma-1* non-complementation screen. Briefly, *fem-1(hc17ts)*IV; *unc-42(e270)*V L4 larvae, which develop as females when raised at 25°C (Nelson et al., 1978), were mutagenized with EMS or psoralen/UV (Yandell et al., 1994) and crossed to *sma-1(mu83)*/+ or *sma-1(e30)*/+ males; progeny from this cross were screened for the Sma phenotype. Potential *sma-1* mutants were crossed to N2 males; animals homozygous for the new *sma-1* allele were obtained by picking Unc Sma animals among the F_2 progeny of this cross. All *sma-1* mutants isolated were recessive and did not show a maternal effect (data not shown).

A migration assay was used in some *sma-1* noncomplementation screens. Unlike wild-type animals, newly hatched *sma-1* L1 larvae fail to chemotax to their food source, *E. coli*. (V. Praitis and J. Austin, unpublished data). L1 larval progeny from *fem-1(hc17ts)*; *unc-42(e270)* female × *sma-1(e30)*/+ male crosses were placed at the center of 60 mm NGM plates seeded with *E. coli* at their perimeter. During a 1 hour incubation at 20°C, most non-Sma larvae migrated to the *E. coli* lawn; animals remaining at the center of the plate were screened for the Sma phenotype.

Immunofluorescence

Animals were fixed and stained by a modification of the method described by Kenyon (1986). Embryos or larvae were placed on polylysine-coated microscope slides, coverslips placed on top and frozen on dry ice. After removal of the coverslip, slides were fixed in –20°C methanol (7 minutes) and –20°C acetone (7 minutes) and rehydrated in an ethanol series (90%, 60%, 30%; 2 minutes each) followed by PBS (150 mM NaCl, 10 mM $NaPO_4$, pH 7.4). Slides were incubated with either MH27 (Francis and Waterston, 1991) or 9.2.1 (Miller et al., 1986) monoclonal antibodies followed by rhodamine-conjugated goat anti-mouse IgG (Cappel). Incubations were at 37°C in PBS/1% BSA/1% normal goat serum. Slides were mounted using 2% N-propyl gallate in 80% glycerol/20% PBS.

Comparison of wild-type and *sma-1* larval development

We determined brood size by counting eggs laid by individual hermaphrodites (N2, *n*=5; *sma-1(ru7)*, *n*=8; *sma-1(e30)*, *n*=8; *sma-1(ru18)*, *n*=9). Egg counting continued until no eggs were laid in a 16 hour period. Some *sma-1* hermaphrodites had an Egl (egg laying defective) phenotype that resulted in internal hatching of eggs. In this case, larvae and unhatched eggs contained in the hermaphrodite were also counted. Percentage hatching was determined by allowing approx. 30 gravid hermaphrodites to lay eggs for 1-3 hours, incubating eggs for 15 hours at 20°C and counting unhatched eggs. Total number eggs tested: N2, *n*=247; *sma-1(ru7)*, *n*=222; *sma-1(e30)*, *n*=265; *sma-1(ru18)*, *n*=195.

To determine time required to reach adulthood at 20°C, we used eggs laid in a 2-3 hour period; hatched larvae were counted 24 hours later. Plates were examined every 8-12 hours for up to 7 days to determine when each animal molted to become an adult. Number of larvae examined: N2, *n*=138; *sma-1(ru7)*, *n*=82; *sma-1(e30)*, *n*=108; *sma-1(ru18)*, *n*=123. The percentage of animals that reached adulthood was calculated as number of larvae that became adults within 7 days divided by the number of larvae present 24 hours after egg-laying.

Length measurements of embryos and larvae

To measure changes in length during morphogenesis, embryos were placed on agar pads in Egg Buffer (Edgar, 1995), coverslips placed on top and sealed with microscope oil, and viewed using Nomarski microscopy. For each time point, a video recording of multiple focal planes was made. Embryo length was determined from the recording using a Scalemaster II digital ruler. T=0 was start of division of the AB blastomere. Length measurements were made every 30 minutes from T=4 hours until T=12 hours. To compare wild-type and *sma-1* elongation rates, comma-stage embryos were videotaped as described above. T=0 was when the embryo reached 1.5-fold stage. Length measurements were made every 30 minutes for 2.5 hours.

Length measurements of newly hatched larvae (within 1 hour of hatching) were made as described above. Three body regions were measured: head (tip of nose to posterior end of pharynx), body

(posterior end of pharynx to anal opening) and tail (anal opening to tip of tail) (Fig. 1A). Total body length was calculated as the sum of the three measurements. The percentage increase in body length during larval development was calculated by comparing the length of molting L4 larvae, measured as described above, with that of newly hatched larvae.

Comparison of embryonic development in *sma-1* and wild-type embryos

N2 and *sma-1(ru18)* embryos were placed on agar pads and incubated at 20°C. T=0 was start of division of the AB blastomere. In the first experiment, we determined when embryos reached the 26-cell stage (designated to be when the P_3 blastomere completed its cell division to form D and P_4) and when body-wall muscles began to twitch. In a second experiment, embryos were videotaped at 30 minute intervals starting at T=10 hours to determine the start of pharyngeal cuticle formation and of pharyngeal pumping. Formation of pharyngeal cuticle was scored based on increased refractivity at the lumenal surface of the terminal bulb (Sulston et al., 1983).

Cloning and sequencing *sma-1*

sma-1(mu83) hermaphrodites were transformed with genomic clones by germ-line DNA injection; pPD10.46, which expresses a partial *unc-22* antisense transcript, was used as a coinjection marker (Fire et al., 1991). A pool of five cosmids (T04A9, C10C2, R07A10, F09F2 and C52E4) rescued the *sma-1* phenotype. In transformations with individual cosmids (K12G11, T04A9, C10C2 and R07A10) only C10C2 rescued the *sma-1* phenotype. Concentration of injected cosmids was 0.1 μg/μl. Transformation with 0.1 μg/μl pAZ9 did not rescue the *sma-1* phenotype; transformation with 0.8 μg/μl produced three independent lines in which the *sma-1* phenotype was rescued.

Antisense RNA transcripts for germ-line injection were generated by in vitro transcription of pAZ4 (Fig. 5C) (Megascript, Albion, Austin, Texas) and purified using GlasPac (National Scientific). 4/5 hermaphrodites injected with 1 μg/μl *sma-1* RNA produced progeny that matched the *sma-1* mutant phenotype. The percentage of *sma-1* phenocopies produced by each hermaphrodite varied from 33% to 89% of total progeny; brood sizes varied from 104 to 236. The remaining injected animal had a small number (17) of only wild-type progeny.

The *sma-1* gene product was initially identified by partial sequencing of pAZ9; the complete genomic sequence of the *sma-1* locus was provided by the *C. elegans* Genome Consortium (Waterston and Sulston, 1995). Sequences shown are based on the genomic sequence; intron locations were determined by comparison with *sma-1* cDNA sequences. *sma-1* cDNAs were obtained by screening oligo-dT and random-primed *C. elegans* cDNA libraries (libraries provided by L. Miller (Rhind et al., 1995) and R. Barstead). Two *sma-1* cDNA clones, yk96e11 and cm18c11, were identified from collections of *C. elegans* Expressed Sequence Tag (EST) cDNA clones. A 685 bp region of the *sma-1* coding sequence, encoding amino acids 2481-2708, was not covered by any of our *sma-1* cDNAs. Inspection of *sma-1* genomic sequence and comparison with the corresponding β_H-spectrin protein sequence indicated that this region did not contain an intron. An alternative splice was observed near the 3′ end of the gene, which removed nucleotides 11535-11864 from the sma-1 cDNA sequence, corresponding to amino acids 3846-3955. The GenBank accession number for the *sma-1* cDNA sequence is AF053496.

The extent of the *sma-1(ru18)* deletion was determined by PCR amplification and sequencing of the deletion breakpoint. Sequencing of four independent subclones from a PCR reaction gave identical results: the *sma-1(ru18)* deletion removes 1703 bp of *sma-1* coding sequence and a 48 bp intron, and at the site of the deletion, an additional 28 bp of sequence are inserted that do not match sequences elsewhere in the *sma-1* gene. As a result, there is a frameshift in the *sma-1(ru18)* coding sequence relative to the wild-type sequence; the predicted *sma-1(ru18)* gene product would contain the initial 208 amino acids of SMA-1, plus 23 novel amino acids before premature termination of translation at the first stop codon.

RNA isolation and northern analysis

Total RNA was prepared from mixed-stage embryos by extraction with phenol and guanididium thiocyanate (RNA STAT-60, Tel-Test 'B' Inc., Friendswood, TX), separated by formaldehyde gel electrophoresis and transferred to nylon membrane in 10× SSC. To allow comparison of *sma-1* and *myo-2* hybridizations, 40 μg samples of total RNA were split and run on two halves of a single gel. After transfer, one half of the membrane was hybridized with each probe. Hybridization of membrane-bound RNA was carried out using the Genius system of Digoxigenin (DIG)-based nucleotide detection (Boehringer-Mannheim). *sma-1* (pAZ4) and *myo-2* (pJK191) transcribed RNA probes were prepared using 30% DIG-11-UTP:70% UTP.

In situ hybridization

Subclones from *sma-1* (pAZ4) and *unc-54* (pTR128) were used to make DIG-labeled single-stranded DNA probes (Patel and Goodman, 1992). In situ hybridization was carried out by a modification of the method described by Seydoux and Fire (1994). Solutions and the method of alkaline phosphatase-mediated detection were as previously described. In our modified protocol, after formaldehyde fixation and hybridization, embryos were washed for 30 minutes at 48°C in each of the following solutions: Hyb; 3 parts Hyb/2 parts PTw; 1 part Hyb/4 parts PTw; PTw. Embryos were then washed for 30 minutes in PBT at room temperature prior to alkaline phosphatase-mediated detection. Primary identification of fixed and hybridized embryos at different stages of morphogenesis was based on embryo shape. For embryos in early morphogenesis, the distinctive morphology of the epidermal cells was used to determine embryo orientation and the extent of epidermal enclosure. Identification of the *sma-1* RNA-expressing cell in the ventral head region as the excretory cell was based on comparison of the location of the stained cell in fixed embryos with the location of the excretory cell in living embryos at several different stages of embryonic development.

RESULTS

Mutations in the *sma-1* gene alter *C. elegans* morphology

In the *C. elegans* embryo, early cell proliferation is followed by a period of morphogenesis during which the embryo undergoes a fourfold elongation (Sulston et al., 1983) (Fig. 1A). At hatching, wild-type *C. elegans* larvae are long and thin with a pointed nose and tapering tail (Figs 1B, 2A). In contrast, we found that larvae homozygous for mutations in the *sma-1* gene are short and wide with a blunt nose and a crooked tail (Fig. 2C,D). The severity of this phenotype varies between *sma-1* alleles. Three *sma-1* alleles, *sma-1(ru7)*, *sma-1(e30)* and *sma-1(ru18)*, described in detail in this paper, represent the range of phenotypes observed. When we measured newly hatched larvae, we found that homozygotes for each *sma-1* mutation had a characteristic length (Table 1). The mildest allele, *sma-1(ru7)*, reduced body length by 27% relative to wild type (Fig. 2C); homozygotes of a moderate allele, *sma-1(e30)*, were 39% shorter than wild type. The allele that produced the most severe phenotype, *sma-1(ru18)*, reduced body length by 44% and appears to be a *sma-1* null allele (see below) (Fig. 2D). The decreased length of *sma-1* mutants is not due to a defect in a single body region. Comparing the head, central body and tail regions in wild-type and *sma-1* larvae, we found

a proportionate decrease in the length of each body region (Fig. 1B; Table 1).

Additional morphological phenotypes are observed in *sma-1* mutants. The pharynx, a neuromuscular tube that forms the first portion of the *C. elegans* digestive tract, is dramatically altered in *sma-1* mutants. The pharynx contains four regions that can be easily distinguished in wild-type animals: the procorpus and isthmus are narrow and elongated, while the metacorpus and terminal bulb are globular (Albertson and Thomson, 1976) (Figs 1B, 2B). In *sma-1* mutants, all four pharyngeal regions are present but the procorpus and isthmus fail to elongate (Fig. 2E). In addition, the cuticle of *sma-1* mutants is twisted and the excretory cell canal, required for osmotic regulation, is short and abnormally shaped (M. Buechner and E. Hedgecock, personal communication).

In spite of their morphological defects, all of the *sma-1* mutants we examined are both viable and fertile as homozygotes (Table 2). *sma-1* mutants have a smaller brood size than wild type, but *sma-1* and wild-type eggs have a similar rate of hatching. In *sma-1* mutants with a severe phenotype, such as *sma-1(ru18)*, larval development takes place more slowly than normal and although most animals eventually become adults, some are pale, thin and do not lay eggs (Table 2).

sma-1 mutants elongate more slowly than wild-type embryos

By comparing the development of wild-type and *sma-1* embryos, we found that *sma-1* embryos do not elongate normally. Early development of *sma-1* embryos appeared normal: both wild-type and *sma-1* embryos reached the 26-cell and comma stages at similar times (Fig. 3A-D). During morphogenesis, however, *sma-1* embryos did not increase in length to the same degree as wild-type embryos (Fig. 3E,F). To determine if abnormal morphogenesis of the *sma-1* embryos was due to an alteration in epidermal cell number or pattern, we used MH27, a monoclonal antibody that recognizes the apical junctions of *C. elegans* epidermal cells (Francis and Waterston, 1991). We found that the number and arrangement of epidermal cells in *sma-1* embryos was the same as that in wild-type embryos (Fig. 3G,H). The *sma-1* elongation defect is specific to embryogenesis: during larval development, the percentage increase in length for *sma-1(ru18)* and wild-type animals is similar (Table 2).

To determine the nature of the elongation defect in *sma-1* embryos, we measured the progressive change in length during morphogenesis in wild-type and *sma-1* embryos (Fig. 4A). We found that wild-type and *sma-1* embryos elongate for the same period of time, but that the rate of elongation was decreased in the *sma-1* mutants. Elongation of wild-type and *sma-1* embryos began at the same time, about 4.5 hours after the first cell division. Between the comma and 1.5-fold stages (6-6.5 hours), wild-type and *sma-1* rates of elongation diverged, with the *sma-1* embryos elongating more slowly than wild type. For both wild-type and *sma-1* embryos, significant elongation ceased between 9 and 10 hours after the first cell division. Because the wild-type and *sma-1(ru18)* embryos elongated for similar periods of time, we conclude that the decreased elongation rate of the *sma-1* embryos is the primary cause of their mutant phenotype.

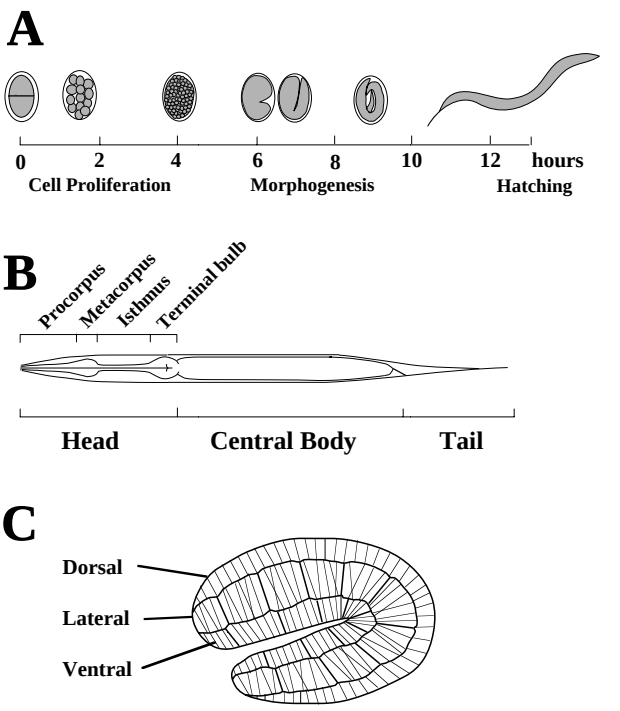

Fig. 1. (A) *C. elegans* embryogenesis lasts 13 hours at 20°C and can be divided into three periods: cell proliferation, morphogenesis, and a final period of cell differentiation and cuticle formation (Sulston et al., 1983). The diagram shows stages of embryogenesis, from left to right: 2-cell; early cleavage; late cleavage; comma; 2-fold; late morphogenesis; newly hatched larva. During morphogenesis, different stages can be distinguished by embryo shape: lima bean stage embryos have a small ventral indentation; comma stage embryos have begun to elongate; at 1.5-fold stage, the posterior region of the embryo extends halfway up the length of the egg, and at 2-fold stage, all the way up the length of the egg. (B) Diagram of wild-type *C. elegans* larva at hatching: head, body and tail regions are indicated. The head region contains the pharynx, consisting of two narrow regions (procorpus and isthmus) and two globular regions (metacorpus and terminal bulb) (Albertson and Thomson, 1976). (C) Schematic diagram of epidermal actin fibers in a 2-fold embryo. Thick lines indicate epidermal cell boundaries, thin lines represent actin fibers; actual number of actin fibers is greater than that shown. In the dorsal and ventral epidermis, actin fibers are parallel and located just under the apical membrane. Actin fibers are also observed in the lateral epidermis (Priess and Hirsh, 1986; Costa et al., 1997), but their precise arrangement has not been determined; one possible pattern is shown.

Different *sma-1* mutants elongate at different rates

We compared the elongation of different *sma-1* mutants to determine whether differences in elongation rate could account for their differences in length. For each mutant the change in length was measured every 30 minutes over a 2.5 hour period starting at the 1.5-fold stage; our previous experiments had shown that this is the period of most rapid elongation (Fig. 4B). The most linear period of elongation was between 0.5 and 2.0 hours after the 1.5-fold stage; for each *sma-1* mutant we calculated an elongation rate by linear regression of the data from this 1.5 hour period (Table 3). We found that all of the *sma-1* mutants elongated at a slower rate than the wild-type embryos and that for each *sma-1* allele, the rate of elongation

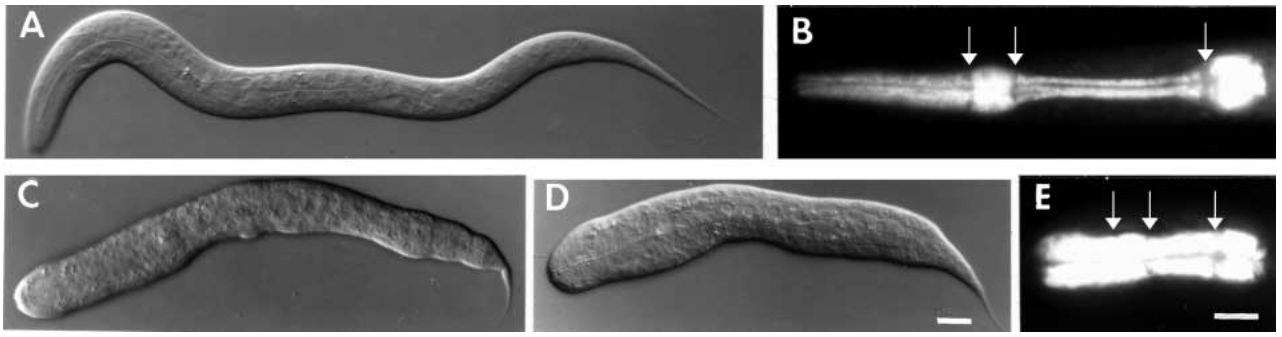

Fig. 2. *sma-1* mutants are shorter than wild-type animals at hatching. Wild type (A), *sma-1(ru7)* (C) and *sma-1(ru18)* (D) larvae were photographed within 1 hour of hatching. The *sma-1* mutants are shorter and broader than wild type, with a rounded head and a short crooked tail. To compare pharyngeal morphology, wild-type (B) and *sma-1(ru18)* (E) L1 larvae were stained with 9.2.1, a monoclonal antibody that recognizes pharyngeal myosin (Miller et al., 1986). Arrows indicate boundaries between regions of the pharynx described in Fig. 1A. Bar in D, 10 μm (also applies to A,C); bar in E, 10 μm (also applies to B).

corresponded to the severity of its mutant phenotype (Table 1; Table 3).

To rule out the possibility that the decreased elongation rate of *sma-1* mutants was due to a decrease in the overall rate of embryonic development, we compared timing of developmental events in wild-type and *sma-1* embryos. We chose events that span *C. elegans* embryogenesis: formation of the 26-cell embryo, first twitch of the body wall muscles, deposition of pharyngeal cuticle and start of pharyngeal pumping, which occurs just prior to hatching. We found that all four events took place at similar times in wild-type and *sma-1(ru18)* embryos (Table 4). The similar timing of these events in wild-type and *sma-1* embryos indicates that the decreased elongation rate of *sma-1* embryos is not due to a change in the rate of embryonic development. In particular, we found that the period between the first twitching of the body wall muscles, which occurs just at the start of elongation, and deposition of the pharyngeal cuticle, which occurs shortly after the end of elongation, was similar in wild type and *sma-1* mutants. This result demonstrates that during the period of embryonic elongation, *sma-1* embryos develop at a normal rate.

sma-1 encodes a homolog of *Drosophila* β_H-spectrin

We used transformation rescue to identify genomic DNA containing the *sma-1* gene. Previous mapping data showed that *sma-1* is located on Chromosome V; 3-factor crosses failed to separate *sma-1* from a cloned gene, *osm-6* (Starich et al., 1995). Germ-line transformation with the cosmid C10C2, which contains genomic DNA located near the *osm-6* locus, rescued the phenotype of *sma-1(mu83)* mutants (Fig. 5B; see Materials and Methods). Transformation with either K12G11 or R07A10, two cosmids that overlap C10C2, did not rescue the *sma-1* phenotype.

To test whether *sma-1* was located in the region of C10C2 not included in either K12G11 or R07A10, *sma-1(mu83)* animals were transformed with pAZ9, an 11 kb *Bam*HI subclone of C10C2 (Fig. 5B). Germ-line injection of 0.1 μg/μl pAZ9 DNA had no effect, but injection of 0.8 μg/μl pAZ9 rescued the *sma-1* mutant phenotype (see Materials and Methods). Initial sequencing showed that pAZ9 contained coding sequence for a member of the spectrin family of cytoskeletal proteins (Winkelmann and Forget, 1993). The ability of pAZ9 DNA to rescue the *sma-1* phenotype, but only at a high concentration, suggested that this subclone contained part but not all of the *sma-1* gene.

We confirmed that pAZ9 contained coding sequence for the *sma-1* gene product using RNA-mediated interference. In *C. elegans*, germ-line injection of either sense or antisense RNA into wild-type animals can result in progeny that phenocopy the mutant phenotype of the gene from which the RNA was transcribed (Guo and Kemphues, 1995). Although the mechanism underlying this phenomenon is not yet understood, it has been observed for a number of genes (Rocheleau et al., 1997). When we injected RNA transcribed from a region of potential *sma-1* coding sequence (pAZ4, Fig. 5C) into wild-type animals, 33-89% of the progeny had the characteristic *sma-1* phenotype: decreased length, increased width and a blunt nose (see Materials and Methods).

The *sma-1* protein (SMA-1) coding sequence was determined by comparing genomic sequences from the region

Table 1. Length defects in newly hatched *sma-1* mutant larvae

	Length at hatching[a] (μm)					
Genotype	Total	% Wild type	Head[b]	% Wild type	Tail[c]	% Wild type
Wild type (N2)	245±6	100	78±2	100	55±2	100
sma-1(ru7)	178±6	73	56±4	72	36±2	66
sma-1(e30)	150±7	61	45±2	58	34±3	62
sma-1(ru18)	137±11	56	41±3	53	32±2	58

[a]Larval lengths were measured within 1 hour of hatching.
[b]The length from the tip of the nose to the posterior end of the pharynx.
[c]The length from the anus to the end of the tail.

Table 2. Life cycle of *sma-1* mutants

Genotype	Brood size[a]	% Hatched eggs	% Adults[b]	Time to adult[c] (days)	% Increase in length as larvae[d]
wild type (N2)	321±23	100	100	2.0±0.1	357
sma-1(ru7)	289±38	98	94	2.2±0.6	n.d.
sma-1(e30)	125±93	97	99	3.0±0.7	n.d.
sma-1(ru18)	189±46	98	95	3.5±0.8	442

[a]Average number of eggs ± s.d. produced by one hermaphrodite.
[b]Percentage of animals that undergo the L4 molt within 7 days.
[c]Average number of days ± s.d. from egg laying to L4 molt.
[d]Percentage increase in length from hatching to L4 molt; n.d., not determined.

of the *sma-1* gene with a series of overlapping cDNAs (Fig. 6; Kershaw, 1996; Lennard, 1997; see Materials and Methods). pAZ9 contains a majority of the *sma-1* coding sequence, but lacks both its 5′ and 3′ ends (Fig. 5C); the mechanism by which injection of pAZ9 DNA at a high concentration rescues the *sma-1(mu83)* phenotype is presently unknown. Using Southern analysis we found that this locus was altered in several *sma-1* alleles. *sma-1(ru18)* and *sma-1(ru19)* contain deletions near the 5′ end of the *sma-1* gene (Fig. 5C; data not shown). Sequencing across the *sma-1(ru18)* deletion breakpoint confirmed that there is a 1.8 kb deletion in this mutant that creates a frameshift in the *sma-1* coding sequence (see Materials and Methods). Two other alleles, *sma-1(ru13)* and *sma-1(ru16)*, also had altered patterns of *sma-1* genomic DNA restriction fragments (data not shown).

SMA-1 is a 4063-amino-acid protein that contains 30 copies of the 106-amino-acid spectrin repeat (Fig. 6). In addition, SMA-1 contains an N-terminal actin-binding domain, an SH3 domain and a C-terminal pleckstrin homology (PH) domain. The two major classes of spectrin proteins, α- and β- spectrins, can be distinguished by their arrangement of spectrin repeats and other protein domains (Winkelmann and Forget, 1993) (Fig. 7A). Comparing SMA-1 with previously identified spectrins we found that its pattern of protein domains was identical to that of β_H-spectrin, a novel β-spectrin isoform identified in *Drosophila* (Dubreuil, 1990; Thomas et al., 1997) (Fig. 7B). Alignment of the SMA-1 and β_H-spectrin sequences gave 37% amino acid identity (data not shown).

SMA-1 and β_H-spectrin share features that distinguish them from other identified β-spectrins. SMA-1 and β_H-spectrin each contain 30 spectrin repeats rather than the 17 spectrin repeats found in conventional β-spectrins; both proteins also contain an SH3 domain not found in other β-spectrins. For conventional β-spectrins, binding to ankyrin is an important means of membrane attachment; in SMA-1 and β_H-spectrin, sequences required for β-spectrin to bind ankyrin (Kennedy et

Table 3. Elongation rate of wild-type and *sma-1* embryos

Genotype	Rate of elongation[a] (μm/hour)
Wild type (N2)	51±5
sma-1(ru7)	28±8
sma-1(e30)	20±3
sma-1(ru18)	10±4

[a]Rates were derived from the measurements of elongating embryos described in Fig. 4B. Length measurements were made every 30 minutes over a 2.5 hour period. Rates shown were derived by linear regression of the central four data points (0.5-2.0 hours). For each mutant the elongation rates of individual animals were determined and then averaged. Wild type (N2), *n*=7; *sma-1(ru7)*, *n*=8; *sma-1(e30)*, *n*=8; *sma-1(ru18)*, *n*=9. The average correlation coefficient for each mutant was ≥0.96.

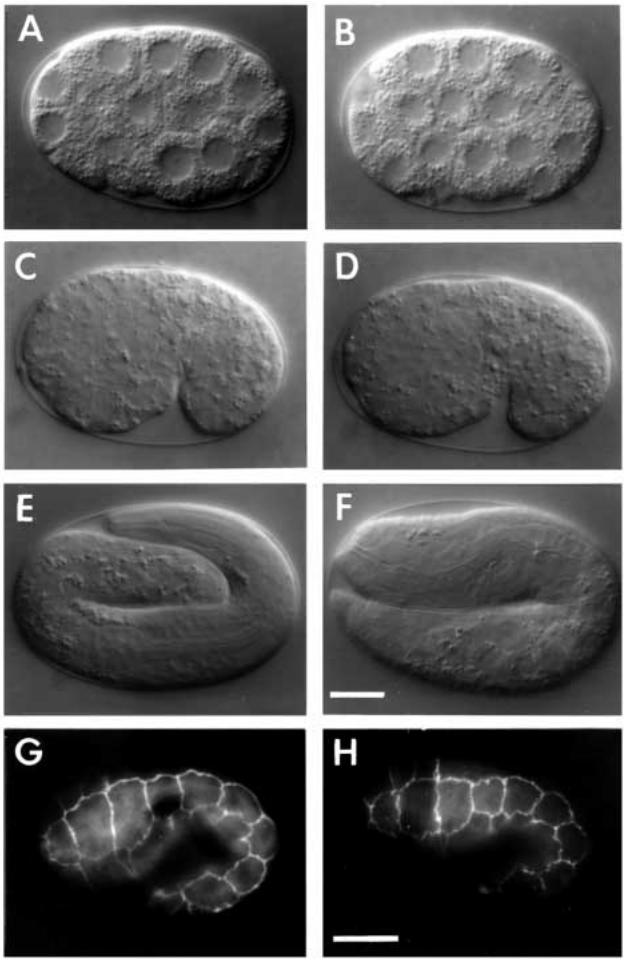

Fig. 3. Elongating wild-type and *sma-1* embryos. Wild-type (A,C,E) and *sma-1(ru18)* (B,D,F) embryos were photographed at 1 hour (A,B), 7 hours (C,D) and 11 hours (E,F) after the 2-cell stage. During cell proliferation (A,B) and early morphogenesis (C,D) wild-type and *sma-1* embryos appear similar. However, by the time wild-type embryos (E) reach the 4-fold stage, *sma-1(ru18)* embryos (F) are significantly shorter. (G-H) Wild-type (G) and *sma-1(ru18)* (H) 1.5-fold embryos stained with MH27 monoclonal antibodies, which recognize the apical cell junctions of epithelial cells, including the epidermis (Francis and Waterston, 1991). Embryos are dorsal side up and anterior to the left; in each embryo the pattern of lateral epidermal cells can be seen. Bar in F, 10 μm (also applies to A-E); bar in H,10 μm (also applies to G).

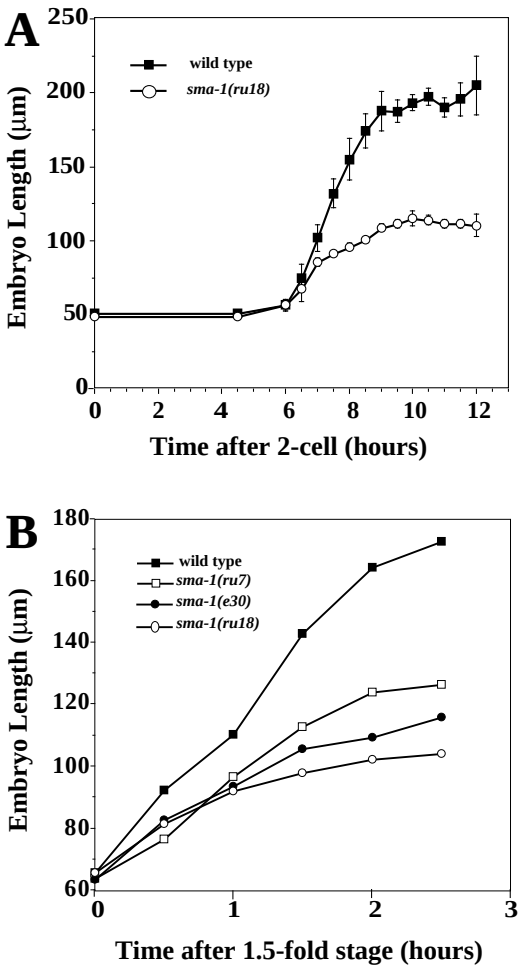

Fig. 4. Elongation rate is decreased in *sma-1* mutants. (A) Lengths of wild-type (■) and *sma-1(ru18)* (○) embryos were measured every 30 minutes for 12 hours starting at the 2-cell stage. Wild-type and *sma-1(ru18)* embryos begin to elongate at the same time, but their elongation rates diverge by the 1.5-fold stage. Wild type, *n*= 4; *sma-1(ru18)*, *n*=3. Data shown are mean ± s.d.; for some data points standard deviations were small and error bars are not visible. (B) Length of wild type (■), *sma-1(ru7)* (□), *sma-1(e30)* (●), and *sma-1(ru18)* (○) embryos were measured every 30 minutes for 2.5 hours starting at the 1.5-fold stage. For each strain, 7-9 animals were measured. Data shown are for representative single animals.

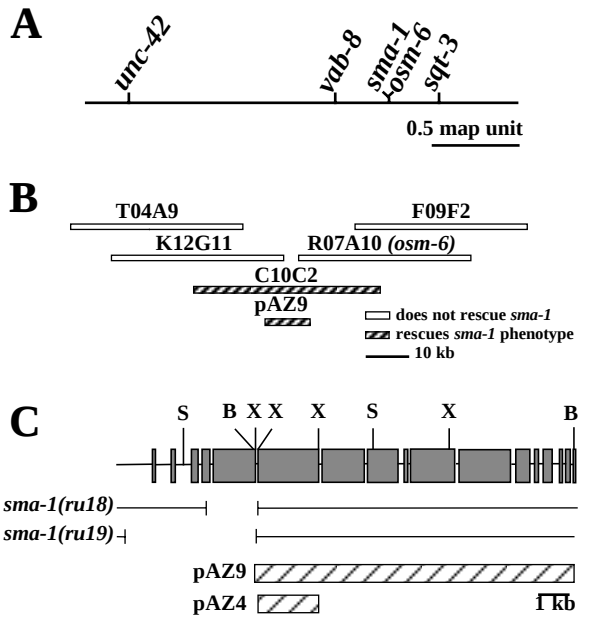

Fig. 5. Cloning *sma-1*. (A) *sma-1* is located in the central region of Chromosome V. (B) Cosmids mapped to the *osm-6* region of Chromosome V were tested for their ability to rescue the *sma-1* mutant phenotype (see Materials and Methods). In tests of individual cosmids, only C10C2 showed rescuing activity; pAZ9, an 11 kb *Bam*HI subclone of C10C2, rescued the *sma-1* mutant phenotype when injected at a high concentration. (C) The *sma-1* locus. Exons are indicated by boxes; *Bam*HI (B), *Sph*I (S) and *Xho*I (X) restriction sites are indicated. Location of deletions in *sma-1(ru18)* and *sma-1(ru19)* are shown as gaps in the lines below the restriction map. Regions of genomic DNA contained in pAZ4 and pAZ9 are shown at the bottom.

al., 1991) are poorly conserved. *Drosophila* β-spectrin has 65% amino acid identity with a consensus sequence of β-spectrin ankyrin-binding domains (Dubreuil et al., 1990; Thomas et al., 1997), but comparing SMA-1 and β_H-spectrin with this consensus sequence gave only 28% and 39% amino acid identity, respectively (Fig. 6B; Thomas et al., 1997). Based on their identical organization and distinctive differences from other β-spectrins we propose that *sma-1* is the *C. elegans* homolog of *Drosophila* β_H-spectrin.

sma-1 is specifically expressed at the start of morphogenesis

sma-1 probes recognize a band of approximately 14 kb on northern blots of total embryonic RNA (Fig. 8). In RNA isolated from the two *sma-1* deletion mutants, *sma-1(ru18)* and *sma-1(ru19)*, the *sma-1* message was decreased both in size and abundance relative to wild type. In *C. elegans*, premature termination of translation is correlated with an increased rate of mRNA turnover (Pulak and Anderson, 1993). Therefore, the decreased level of *sma-1* message may be due to frameshifts introduced by the deletions in *sma-1(ru18)* and *sma-1(ru19)*.

Using whole-mount RNA in situ hybridization, we found that *sma-1* transcripts are present in the embryonic epidermis at the start of morphogenesis (Fig. 9). In a population of mixed-stage embryos hybridized with a *sma-1* antisense probe, *sma-1* RNA was not observed in pre-morphogenesis embryos. In particular, there was no sign of *sma-1* transcripts in early cleavage-stage embryos (2-8 cells), indicating that maternal *sma-1* RNA is not contributed to the embryo (data not shown). At the start of morphogenesis, the cells of the epidermis form a patch on the posterior dorsal surface of the embryo and then spread ventrally and anteriorly to enclose the embryo (Priess and Hirsh, 1986; Williams-Masson et al., 1997). In embryos just beginning morphogenesis, *sma-1* RNA was present in cells along the dorsal surface of the embryo, corresponding to the location of the epidermis at this point in development (Fig. 9A).

Examining embryos at successive stages of morphogenesis, we found that the location of the *sma-1* RNA changed in a pattern that exactly matched the movements of the migrating epidermal cells. During early morphogenesis, when the epidermal cell sheet spreads over the lateral surfaces of the

A

```
 1 MRYYEMQVRVPTSGAPPVRADANGTDQDEFNNETLYFERSRIRTLQDERVHIQKKTFTKWCNSFLNRASLEIVDLFEDVGDGIMLMKLLEIISGDKLGKPNRGRMRVQKVENL
   NKVLDFLKKKKIQLENIGAEDILDRNERLILGLIWTIILRFQIDTIVIEDEEERGERKHAKDALLLWCQRKTAGYPNVRIENFTTSWRNGLAFNALIHSHRPDLVDFNRLNPN
   EHVDNLNHAFDVAEKKLEIARLLDAEDVDVTRPDEKSIITYVSLYYHHFAKQKTEMTGARRIANIVGKLMVS

 2 ETMEDDYEHIASELLNWIRVTIKTLESRRFPN.SLNGMREEHAKFNQFRTSEKPPKYKEKGELEALFFTIQTKRKAMSRKQYQPPQGLFMHDIESAWAQLDYAENERQVAIIAELQRQEKL
 3 EQLAQRFHKKAKLRDSWLRSVQVVLEEMEHGR....SASQVEKTLKKQQAISTDILARED.RFKMLTAMCNELCTE.KYHESDKVRGM.EREIIDRWTQLLTLLEQRKRALMS
 4 LNDLMSLLRDIDTLSNELYSLEPAVRNRDVGK....HLIGVEDLLGKHDLLDAQINAHGS.LLSKLSQSANNYIRH.KEEQFDVLQRK.LDEVTAQYNTLVELCRSRRLGLER
 5 ARSLFQFVQDHEEEMAWLAEKEKLCTTALNSG....DISAVPQTTLLYKNVEMEMQTHWA.RSKGMIAGGERLVQNGQS. KEDIQRR.LTQMNHRWERLRVAVDALGNWLSE

 6 ARHAQQYFQDANEAESWIREKMPLVKSDDLGRDEGAAESLLQRHARLEEEIRAYKSDISRLEEMQSQLANSAFHTA
 7           TTSQSVQET EEVNVPQVEMSYNYEGNGMRVSKGEVLALLEKSTPEWWRALKRDGTEGYVPANYCKIVPGETVTVTQTTQKTTTTLE
 6                                                                                  GNETKSSVVADRQHKISNDYRELKRLADVRRRLLSD

 8 NIKLLRFYRECDEFERWAKEIEVSLADEP.......SPEHVAAFRRKFDKLEADMKTNGGTQLKHINDIANDLISE.GHGQSRKIEVR.QHKINAMWDNLERLRKQRGVRLEA
 9 TERVADFDTTCESAREWMLSKFEQLDRNPN......DVKSLQNLERDLKPLEDKIAALEKLAAAVKKDHPEEA.........AAIERK.IAELRALHADLLRRAQEKMLLAEQ
10 TQGKEMFESALRDMIGWIEKTRKVMMEDVHPV....DVAEAEELLKKHYELGEQIKDKKY.EVEYCQELGRRLLER.NPRMSK.VEEQ.LQNLVSEMASLRDLYRRRDTILKQ
11 QLDLQLFNRESERIDAATKGHEAFLEFDNLGD....SVESVENLLKRHRDLEAKLDAQEA.RLEAFSRTADDMIKA.QHADSAYIEQR.RRDVLARREAVRRAAAQRKKQLEA
12 SLEYQEMRREADEVVGWMYEKAKLVMSGDDSAL...APSAIPHRLLKHEAFEAEIIANEP.RIQQINSEGDGLVSK.KHYESPNVEKI.VRQVNAQWGDLKKQVWNKGLRLRQ
13 AADQKGLDRILEDAHAKLDEMQTALNSKDQGL....DLRSVKDLLQKHAVLEQEMGLYGN.KLSDIENRGKKMAVD.GHYDADRIHST.VGQLLQRYAAMKGPAQRRKGDLDE
14 SRLWHQLVFDVDCELQWIAEKKPIASSQDCGR....TLTEALNMVKKQEQLEAEVNQHGG.QIDKVLLQAGELIKR.HHSASSQIKAK.SSELETAWSELKKLLRLRRAVVDW
15 GVKEQQYLFDAAEVESWMNEKRNALASEDYGN....DEDAARKLLSKHRALCEDMTTYRQ.WLEKLEVKCVELVES.NRPHVERFQKR.QDELVREFDALSKLAEDRRNALED
16 AVCLYEYMRESADLGQSIEENLRVAMSEEFAE....DYEHLKELQSKFDEFKQKVKNGSE.RFTSCETAANAILRR.NPPFARDVVKK.QEALRTAWNTLCEYIEARDSKLAV
17 AEELHRFHRDVDEFEQWMADK.MANMPRDLGR....DVKHVHSLWQHHEALDKEIHNSQP.RLAKLVEEAERLKKTYPGGNAEQIGGR.QQTLEQEWEELKNATDDRKDMLRA
18 AFDLHTFNGKVRDLLAWTDLTISDIQSDLHIN....DLQQAEWLQTEHSRLSHEMDAREP.EFARLVNDGEKMITA.QHYASEEIKNK.THLLKSALERLRSEWALRNGFLSQ
19 AVQWHAFQREAKQIIASIGSKRTTLRSLAVGG....SVADVESQTKRLDTFEKALSTLDE.RTATLDHTANELMKA.RHMESKNISMW.QSNVHEELKLLRQDIEARHAMLKD
20 AFALASFDSDVAQIEAWIDEKTNGVRKAQDLSSESISIDEKMKRLQTHQALEAEVTANKP VVDQILQRGNQLKNLHRNP...KIANR.CDELSYKWNQLSGACADQSLALEE
21 ARDLLRFKQLVENVLAWINEKEVLVSTADMGK....DMEHCRLLLERLDGTRSDSIVDEQ TLDEINRLGEKLVKQ.GRSSRDQVQKE.QQHLNEKWRLLLGQLAHYRTELLA
22 AMEVHTFNRDVEDTDERIHEKVAAMKSDDYGK....DFASVELLVRKQSALERDMSAIHQ.KLIAHDKDAQKILEK.RPPLRETVLDS.LKKLEESWEQLSKAAELRNEKLNR
23 SFKLYKYLDDVKKVEQWANQVRNKMTSHQTPK....DSNGARKILEQHHERKAEIDGRSE.ELRLLHEEGQALNQE.QPEHKAEVQRA.HKRVQNSEHQLRQTWESEKGTLQK
24 LLEWMLWCDEAVQCEQWLSDKETQVARGELGD....TTDAVEMLIKGHSAFEETVRKQSE.KIDALTKNADALVSG.GNNYRADIVTR.SEEVTARHALLLKSMEKRGHMLED
25 SKKYHEFIRQCGELIIWITAKLQLAYDESFL.....DHTNLRSKLQKHMAFDSELVENEK.RLSTVERQGEQLVTD.NHFMSEQVKAQ.LVELRSGWDELRTKSALKTQRLRE
26 AFELHSLQRKVEDIEKWLDKVEGELSSDDHGR....DILSTELLIKKLDTLQTEIAGRSD.AVVEMMKKARELRVQ.GSAAADDCLKQ.AEQVEARYSGLDEPVQIRRENLVD
27 AQAFFQWVKAAEEDLEWLSDRMMLASSGESGD....SLQSALSLQKKHATLEKELDTRQS.AMNDTEQRGKDMIRQ.RHFASTHIQKI.LDRLSSAMLTLKESCGLRRDLLQE
28 AIDAHEYYTEETEAEQWLREQMPLAMSQEMGR....DQAGAESHLRRLTVLDKEVELFKN.EIDRLKKRADGLLAR.EHHDAMSIAAK.QRKLELRHALFGDLCRECARRRTQIVD
29 ASKYHKFVRQADDLSDWLREKERSASAEDYGQ....DLEDCQQIIEQFESTVRELAAAGE.RVAAVQRAQEDLLRS.GHPYGASITAK.GADVQRLWTHVNEVANERKQALNG
30 ARQVHRFDQEADQILNWLQDKEATGVAMEQEDLSRADLASVKAQLQRHDEFMHGMKAVEK.QVAELCHEAERLWNSFPDTR.HHLEVR.RLDMEEQLKDILEAAKKHLEKLRH
31 MQSLQSYFQEYREMMQWMKNMQSTMTSEQLPR....DVASCESLVRRHDEYNLEMQGRKP.FVDDFARQGRRMIQS.SHVLSQEIQEK.VDILEKSWAMLCEIWKDRAELYEE
32 NMDVQKWKQNAEQLDSWLEERAGLLGDDWRMV....DSVEMAETHLRDFDDFLVTLEAQS.EKCDMVKRLTLVEQ

33 NFSRLRSKEIDRARIAEDDQKRRDTIKIVEKGNILANRRQERERRKTQEISLLRPSPSGEEFSTHTMPRKERKDRAKTTADLAPGAIQIGDILASSSTVAPLQSGVEMTKTPS
   FNTRRTQSIRKGSRWEDMGAIDMKGFFDRKQCQQSGGKRATIRSWKNYYGILCGQLLCFFKDEQQFLENVAAAPPVYIYGAQCEQYPEYAKRKNSFRLLLQDGSEFIFSCPDE
   RQMLEWVAKIKFHAHLTPSNQLKSYAYNDDLFQSPDQPPMVAPRRNIGGHDVANRMSHASSVFTTSDDLEQHELDYSRRCSSLPRGKHSGQITMRDCATLPRGFGSDVMEQQP
   TAFFPPSGPLLATPSVLTMSSSSMTANVMPTVVTRKIGVVRRASRRQSVYAESIYGEVEQAIAEANRVSTSRPNGDHAELRHTIQVHPGSSGYTETLMYKEHTSSNYQPMERS
   VSPRNQQNGEFITWVESNQQNQPMNTPDGRSTSASVVSTPSNYDDSDSIKSSSKRKGFGSLFKRGSKHSK
```

B

```
                                20                  40                  60
Consensus       IAEWKDGLNEAWADLLELIDTRTQLLAASYELHKFFHDGKEILGRIDEKHKELPEELGRDASTVE
Dros. β         ......N...S.Q......E....M....R........C.DV....L..QHGVSD......GS.S
Dros. βH        VEKRQEQ.RTS.EN..Q.LNQ.E.K.H.AG.I.R.HR.VA.A.F..QD.NAA.SQ.....LNSAL
SMA-1           VVKKQEA.RT..NT.C.Y.EA.DSK..VAE...R.HR.VD.FEQWMAD.MANM.RD....VKH.H

                          80                  100                 120
Consensus       TLQRVHTAFEHDLQALGVQVQQLQEVAARLQAAYAGDKADAIQNREQEVLAAWQALLDACAGRRV
Dros. β         ....K.YN.LQ..IT.YS....I..ES.K..D.......KE.T.......H..DN.QAM.DA.KQ
Dros. βH        A.L.K.EG..N..V..EA.L.V.V.DSV....K.PSN-.S..AQQQDK.V...ND.KERSTA.GD
SMA-1           S.WQH.E.LDKEIHNSQPRLAK.V.E.E..KKT.P.GN.EQ.GG.Q.TLEQE.EE.KN.TDD.KD
```

Fig. 6. SMA-1 sequence. (A) SMA-1 consists of a series of spectrin repeats interspersed with other protein domains. In this figure, protein domains are numbered based on the nomenclature of Byers et al. (1992). Segment 1, actin-binding domain; segments 2-5, spectrin repeats; segments 6/7, an SH3 domain (segment 7), is inserted into the middle of a spectrin repeat (segment 6); segments 8-31, spectrin repeats; segment 32, partial spectrin repeat required for tetramer formation (Speicher et al., 1993); segment 33, PH domain. For both the SH3 (segment 7) and PH (segment 33) domains, the conserved domain sequence (underlined) is surrounded by sequences not conserved between SMA-1 and β_H-spectrin. (B) Comparison of potential ankyrin-binding domains. A consensus sequence generated by comparison of ankyrin-binding domain sequences from *Drosophila*, mouse and human β-spectrins (Kennedy et al., 1991; Thomas et al., 1997), was compared with corresponding sequences from *Drosophila* β- and β_H-spectrin, and SMA-1. For each sequence, dots indicate amino acids that match the consensus sequence. For SMA-1, this sequence is located in segments 16-17 and is underlined in Fig. 6A.

Table 4. Developmental timing is normal in *sma-1* embryos

Genotype	Time after 2-cell stage of embryogenesis			
	26-cell stage (minutes±s.d.)	First muscle twitch (minutes±s.d.)	Pharyngeal cuticle[a] (hours±s.d.)	Pharyngeal pumping[b] (hours±s.d.)
Wild type (N2)	67±3	364±7	11.0±0.5	12.0±0.5
sma-1(ru18)	69±2	364±7	11.0±0.5	12.0±0.5

[a]Animals were examined every 30 minutes starting at T=10 hours for a change in refractivity in terminal bulb of the pharynx.
[b]Animals were examined every 30 minutes starting at T=10 hours.

embryo, we observed *sma-1*-expressing cells on the dorsal and lateral surfaces of the embryo, but not on the ventral surface or in the head region, which at this stage are not yet covered by the spreading epidermis (Fig. 9B-D). In cross-section, it can be seen that the *sma-1* RNA is located in the outermost cell layer of the embryo (Fig. 9C). As morphogenesis progresses, the spreading epidermis encloses first the ventral surface of the embryo and then the head as the embryo bends ventrally and begins to elongate. In embryos at this stage of morphogenesis, we found a corresponding pattern in which *sma-1* RNA was seen first on the ventral surface (Fig. 9E) and then on the anterior (head) surface of the embryo (Fig. 9F). At the same time, we found that the overall level of *sma-1* RNA rapidly decreased as the embryo began to elongate (compare Fig. 9E-G). *sma-1* RNA in the epidermis was not observed in embryos past the 2-fold stage.

In addition to *sma-1* expression in the cells of the epidermis, we observed a line of *sma-1* RNA in the interior of the embryo, oriented along the anterior-posterior axis (Fig. 9C, E-G). Based on its location, we determined that this *sma-1* RNA is located in the developing digestive tract of the embryo, consisting of the pharynx and intestine (Fig. 1B). During early morphogenesis, it is difficult to determine the anterior extent of *sma-1* staining in the interior of the embryo (Fig. 9C), but as the embryo begins to elongate, the level of *sma-1* RNA increases and at the 1.5-fold stage *sma-1* RNA is clearly present in both the pharynx and intestine (Fig. 9G). A lower level of pharyngeal/intestinal RNA was observed in 2- to 3-fold stage embryos (Fig. 9H). In these older embryos, *sma-1* RNA was also found in the excretory cell and in an unidentified cell near the anus.

The pattern of *sma-1* RNA detected by in situ hybridization points to a stage and tissue-specific pattern of *sma-1* expression in the *C. elegans* embryo during morphogenesis. We observed expression of *sma-1* RNA in several epithelial tissues: epidermis, pharynx, intestine and excretory cell. *sma-1* RNA was not seen in the body wall muscle cells, which are arranged in four stripes underlying the epidermis (Sulston and Horvitz, 1977; Sulston et al., 1983). The highest level of *sma-1* RNA was observed in the epidermis during the early stages of morphogenesis, prior to when differences are observed between development of wild-type and *sma-1* embryos. Thus both the spatial and temporal patterns of *sma-1* expression support the hypothesis that SMA-1 spectrin acts as a component of the epidermal actin cytoskeleton to regulate the morphogenesis of the *C. elegans* embryo.

DISCUSSION

SMA-1 is required for a normal rate of elongation during embryonic morphogenesis

In this study, we have shown that the reduced length of *sma-1* larvae is due to a decreased rate of elongation during embryonic morphogenesis. Although *sma-1* is clearly required for normal morphogenesis, our data indicates that it is not an essential gene. The *sma-1* alleles we have isolated vary in the severity of their elongation defect, but all are viable and fertile including two alleles, *sma-1(ru18)* and *sma-1(ru19)*, that have deletions near the 5′ end of the *sma-1* gene. We sequenced the deletion breakpoint of *sma-1(ru18)* and found that it creates a frameshift in the *sma-1* coding sequence. In northern blots, the level of *sma-1(ru18)* message was decreased relative to wild type, consistent with the presence of a premature stop codon in the *sma-1* coding sequence. In agreement with this result, antisera that recognize the SMA-1 C terminus do not detect protein in *sma-1(ru18)* extracts (V. Praitis, unpublished data). Based on these results, we conclude that *sma-1(ru18)* is a null allele of the *sma-1* gene.

By whole-mount in situ hybridization, we found that *sma-1* RNA is expressed in the embryonic epidermis, supporting previous data that indicated a primary role for the epidermis in

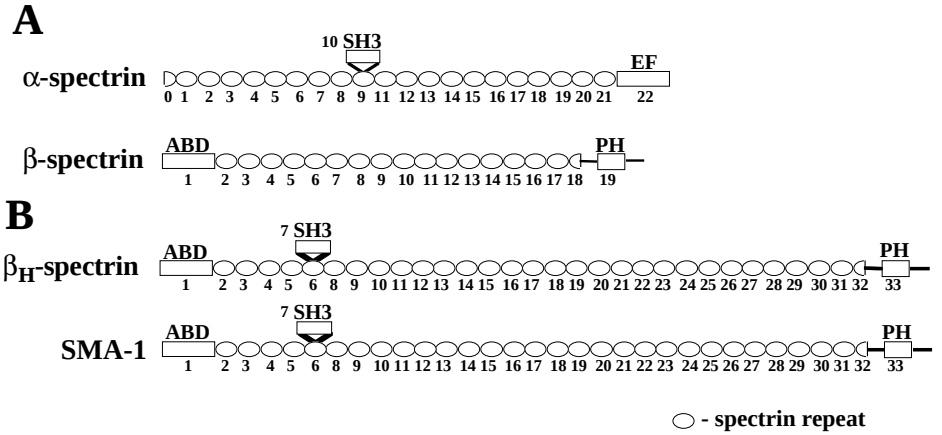

Fig. 7. Spectrin organization. (A) Organization of α- and β-spectrins (Winkelmann and Forget, 1993). (B) The arrangement of protein domains is similar in SMA-1 and β_H-spectrin; both proteins contain a total of 30 spectrin repeats and a similarly located SH3 domain. Thick lines indicate sequences bordering the SH3 and PH domains that do not show sequence similarity between SMA-1 and β_H-spectrin. ABD, actin-binding domain; EF, EF hand domain.

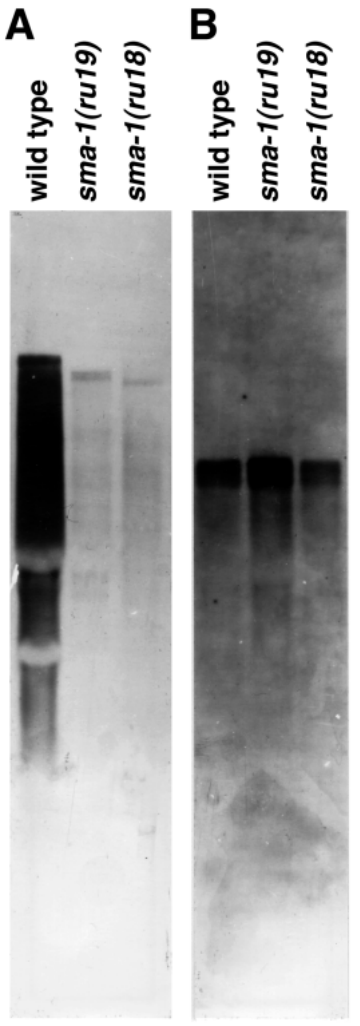

Fig. 8. Comparison of wild-type and mutant *sma-1* mRNAs. Total RNA isolated from wild-type, *sma-1(ru18)* and *sma-1(ru19)* embryos were hybridized with *sma-1* (A) or *myo-2* (B) probes. *sma-1(ru18)* and *sma-1(ru19)* contain deletions in the 5′ region of the *sma-1* coding sequence. In the deletion mutants, *sma-1* message is decreased in size and abundance relative to wild type. In contrast, *myo-2* message abundance was similar for all three samples.

morphogenesis. *sma-1* RNA is first seen in epidermal cells on the dorsal surface of the embryo at the start of morphogenesis and then moves to the lateral and ventral surfaces of the embryo as the epidermal cell sheet migrates over the embryo and encloses it. The level of *sma-1* RNA in the epidermis, as determined by intensity of staining, is high at the start of morphogenesis, but then decreases as the embryo begins to elongate and is undetectable after the 2-fold stage. This pattern suggests that the *sma-1* gene is transcriptionally active in the epidermis for a short period of time early in morphogenesis; it will be interesting to determine whether there is a set of genes required for morphogenesis that are coordinately expressed in the epidermis at this time.

Expression of *sma-1* RNA was also seen in the developing pharynx and intestine. Like the epidermis, both pharynx and intestine are composed of a single cell layer of polarized epithelial cells; however, because these two tissues will form the *C. elegans* digestive tract, the apical surface of these cells faces inwards, towards the future site of the lumen. We found that *sma-1* RNA is located in a thin line that corresponds to the midline of the pharynx and intestine; we propose that this line is created by apical localization of *sma-1* RNA within these cells.

Although *sma-1* mutants develop at a normal rate as embryos, we find that for *sma-1* mutants such as *sma-1(ru18)*, which have a severe phenotype, there are delays in larval development. This phenotype may be due to defects in food intake: in *sma-1* mutants pharyngeal morphogenesis is abnormal and may result in impaired function. In addition, *sma-1* mutants have abnormally shaped excretory cell canals; defects in excretory cell function have been shown to result in slow larval development (M. Buechner and E. Hedgecock, personal communication).

SMA-1 and *Drosophila* β_H-spectrin identify a new class of β-spectrins

The *sma-1* gene encodes a homolog of *Drosophila* β_H-spectrin. The arrangement of protein domains in SMA-1 and β_H-spectrin are identical: actin-binding, SH3 and PH domains are located at the same relative positions and each protein contains the same number of spectrin repeats. These two proteins differ from previously identified β-spectrins in that they contain a greater number of spectrin repeats and an SH3 domain. In addition, a conserved sequence found in conventional β-spectrins, which had been shown to bind ankyrin (Kennedy et al., 1991), is poorly conserved in both SMA-1 and β_H-spectrin. The lack of ankyrin-binding sequence conservation suggests that in SMA-1 and β_H-spectrin this protein interaction domain is either non-functional or binds a protein other than ankyrin. In support of this hypothesis, it has recently been shown that Drosophila β-spectrin, but not β_H-spectrin, is able to bind ankyrin when expressed in Drosophila S2 cells (Dubreuil et al., 1997).

In both *C. elegans* and *Drosophila*, there are genes encoding α-spectrin (Dubreuil et al., 1989; Gattung and Wilson, 1996; K. Norman and D. Moerman, personal communication) and β-spectrin (Byers et al., 1989; Gattung et al., 1996; S. Moorthy and V. Bennett, personal communication) in addition to SMA-1/β_H-spectrin. Drosophila α-spectrin can form heterodimers with either *Drosophila* β- or β_H-spectrin (Dubreuil et al., 1990). In the cell, *Drosophila* α-spectrin colocalizes with both β- and β_H-spectrin, but the two β-spectrin isoforms form non-overlapping domains of membrane-associated cytoskeleton (de Cuevas et al., 1996; Lee et al., 1997; Dubreuil et al., 1997). The distinction between β-and β_H-spectrin localization within the cell is particularly clear in epithelial cells: β_H-spectrin is apically localized, while β-spectrin is found at the lateral plasma membrane (Thomas and Kiehart, 1994). The basis of this difference in location has not yet been determined, but is probably due to the distinctive differences between β- and β_H-spectrin. Apical localization of β_H-spectrin may occur via binding to a ligand of the SH3 domain; conversely, β-spectrin may associate with the lateral membrane via its interaction with ankyrin. We find that *sma-1* RNA is expressed in multiple epithelial tissues in the *C. elegans* embryo. Based on its similarity to β_H-spectrin, we propose that SMA-1 will also be found apically localized in the epithelial cells where it is expressed.

Previous studies suggest that a protein similar to SMA-1 and β_H-spectrin is present in vertebrates as well as invertebrates. Analysis of the chick intestinal brush border identified a

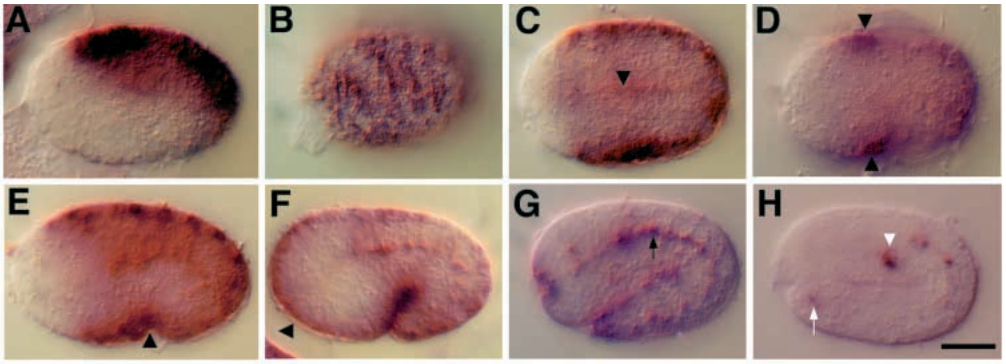

Fig. 9. Location of *sma-1* RNA in *C. elegans* embryos by whole-mount in situ hybridization. Embryos were hybridized with pAZ4 DIG-labeled antisense probe. In all pictures anterior is to the left. (A) Early morphogenesis; lateral view, mid-focal plane, dorsal is at top of photograph. *sma-1* RNA is present in cells on the posterior dorsal surface of the embryo. (B-D) Early morphogenesis (older than A); dorsal view, multiple focal planes of single embryo. (B) Upper focal plane; *sma-1* RNA is present in the cells of the dorsal epidermis. (C) Mid-focal plane; *sma-1* RNA is seen in the outermost layer of cells, except in the region of the head. Arrowhead, early *sma-1* RNA expression in the intestine. (D) Lower focal plane; *sma-1* RNA is seen in a small group of cells on the left and right side of the ventral surface (arrowheads). The position of these *sma-1* expressing cells corresponds to that of the 'leading cells' (Williams-Masson et al., 1997), which initiate ventralward migration of the epidermis and are the first epidermal cells to reach the ventral surface. (E-H) Lateral view; mid-focal plane, dorsal is at top of photograph. By lima bean stage (E), *sma-1* RNA is present on the ventral surface of the embryo (arrowhead); by comma stage (F), *sma-1* RNA is present on the anterior surface of the embryo (arrowhead). *sma-1* expression in pharynx and intestine is most apparent in 1.75-fold stage embryos (G); arrow marks location of boundary between pharynx and intestine. At the 2.5-fold stage (H) *sma-1* RNA is not detected in the epidermis, but is still present in the intestine. Additional *sma-1* expression is seen in the excretory cell (white arrowhead) and an unidentified cell near the anus (white arrow). Bar in H is 10 μm.

spectrin heterodimer, TW260/240, composed of α-spectrin and a large β-spectrin (Glenney et al., 1982). In electron micrographs, TW260/240 tetramers have the same contour length as α/β_H-spectrin tetramers (Glenney et al., 1982; Dubreuil et al., 1990). Intriguingly, experiments that compared the ankyrin-binding capabilities of avian erythrocyte β-spectrin with that of TW260/240, found that erythrocyte β-spectrin bound human ankyrin but that TW260/240 β-spectrin did not (Howe et al., 1985). Although the gene encoding the TW260/240 β-spectrin has not been cloned, its similarities with β_H-spectrin suggest that this is a vertebrate representative of the β_H/SMA-1 class of spectrins.

Role of SMA-1 in *C. elegans* morphogenesis

We find that SMA-1 protein is required to determine cell shape in multiple epithelial tissues during morphogenesis. Mutations in the *sma-1* gene produce defects in the morphogenesis of the epidermis, pharynx and excretory cell. *sma-1* message is expressed in all three of these tissues, as well as in the intestine, at a time when they are undergoing morphogenetic changes in cell shape.

Multiple lines of evidence indicate that elongation of the *C. elegans* embryo during morphogenesis is the result of contraction of apically localized actin fibers in the epidermis (Fig. 1C; Priess and Hirsh, 1986; Wissman et al., 1997; Costa et al., 1998). The *sma-1* gene encodes a homolog of *Drosophila* β_H-spectrin, which in combination with α-spectrin forms tetramers that can cross-link actin. In *Drosophila*, β_H-spectrin is apically localized in polarized epithelia. Our present model is that in the *C. elegans* embryonic epidermis, SMA-1/α-spectrin tetramers form an elastic network that links the actin fibers to each other and to the apical membrane of the epidermis. The presence of this SMA-1-based membrane skeleton would act to stabilize the actin fiber array as the epidermal cells elongate during morphogenesis.

sma-1 mutant embryos elongate at a slower rate than wild type, with each allele exhibiting a characteristic elongation rate. The decreased elongation rates of *sma-1* mutants are consistent with a role for SMA-1 in stabilizing the arrangement of the epidermal actin cytoskeleton. Disruption of a SMA-1-based membrane skeleton might alter the pattern of actin fibers, causing a reduction in the contractile force produced by the actin fibers. Alternatively, SMA-1 may act as an intermediary between the actin cytoskeleton and the plasma membrane, allowing energy created by contraction of the epidermal actin fibers to be converted into cell shape change. In this case, a reduction in SMA-1 activity would reduce the efficiency with which the contractile force is converted into cell shape change.

The SMA-1 sequence suggests a structural role for this protein during morphogenesis; the decreased elongation rate of *sma-1* mutants suggests that this protein also plays a role in regulation of morphogenesis. The newly hatched *C. elegans* larva has a constant diameter, requiring that interactions between the epidermal cells coordinate the process of elongation along the length of the embryo. SMA-1 may be a target of these regulatory interactions or may serve as a cytoskeletal binding site for signal transduction molecules. In addition, there is evidence for regulation of elongation by interactions between tissues in the embryo: in Pat (paralyzed, arrested elongation at two-fold) mutants, which have structural defects in muscle function or attachment, elongation stops prematurely at the 2-fold stage (Williams and Waterston, 1994). Although the *sma-1* mutant phenotype differs from that of Pat mutants, SMA-1 may be a downstream target affected by the muscle-epidermis interaction. Future experiments will clarify the function of SMA-1 in the actin cytoskeleton and allow us to identify proteins that act with SMA-1 to control the process of cell shape change during *C. elegans* morphogenesis.

We thank members of the Austin, Ferguson and Mahowald laboratories for many helpful discussions and for critical reading of the manuscript. We also thank Graham Thomas, Ronald Dubreuil and Mike Costa for sharing results prior to publication. Initial isolation of *sma-1* mutants was carried out in the laboratory of Cynthia Kenyon. cDNA libraries used in this work were provided by Lelani Miller and Robert Barstead; plasmids were provided by Tom Evans and Ed Maryon; monoclonal antibodies were provided by David Miller and

Robert Barstead; the yk96e11 cDNA was provided by Yogi Kohara. DNA sequencing of *sma-1* cDNAs was carried out by the Cancer Research Center DNA Sequencing Facility at the University of Chicago. Some strains used in this work were provided by the Caenorhabditis Genetics Center. Support was provided by ACS grant RPG-98-066-01-DDC, an ACS Institutional Grant to the University of Chicago Cancer Research Center (IRG-41-35) and grants from the Louis Block Fund and the Cancer Research Foundation. V. P. was supported by NIH Training Grant HD07136.

REFERENCES

Albertson, D. G. and Thomson, J. N. (1976). The pharynx of *Caenorhabditis elegans*. *Phil. Trans. Roy. Soc. London* **275**, 299-325.

Bennett, V. and Gilligan, D. M. (1993). The spectrin-based membrane skeleton and micron-scale organization of the plasma membrane. *Ann. Rev. Cell Biol.* **9**, 27-66.

Brenner, S. (1974). The genetics of *Caenorhabditis elegans*. *Genetics* **77**, 71-94.

Byers, T. J., Husain-Chishti, A., Dubreuil, R. R., Branton, D. and Goldstein, L. S. B. (1989). Sequence similarity of the amino-terminal domain of *Drosophila* beta spectrin to alpha actinin and dystrophin. *J. Cell Biol.* **109**, 1633-1641.

Byers, T. J., Brandin, E., Lue, R. A., Winograd, E. and Branton, D. (1992). The complete sequence of *Drosophila* β-spectrin reveals supra-motifs comprising eight 106-residue segments. *Proc. Nat. Acad. Sci. USA* **89**, 6187-6191.

Costa, M., Draper, B. W. and Priess, J. R. (1997). The role of actin filaments in patterning the *Caenorhabditis elegans* cuticle. *Dev. Biol.* **184**, 373-384.

Costa, M., Raich, W., Agbunag, C., Leung, B., Hardin, J. and Priess, J. R. (1998). A putative catenin-cadherin system mediates morphogenesis of the *C. elegans* embryo. *J. Cell Biol.* **141** (in press).

de Cuevas, M., Lee, J. K. and Spradling, A. C. (1996). α-spectrin is required for germline cell division and differentiation in the *Drosophila* ovary. *Development* **122**, 3959-3968.

Dubreuil, R. R., Byers, T. J., Sillman, A. L., Bar-Zivi, D., Goldstein, L. S. B., Branton, D. (1989). The complete sequence of Drosophila α-spectrin: conservation of structural domains between α-spectrin and α-actinin. *J. Cell Biol.* **109**, 2197-2205.

Dubreuil, R. R., Byers, T. J., Stewart, C. T. and Kiehart, D. P. (1990). A β-spectrin isoform from *Drosophila* (β_H) is similar in size to vertebrate dystrophin. *J. Cell. Biol.* **111**, 1849-1858.

Dubreuil, R. R., Maddux, P. B., Grushko, T. A. and MacVicar, G. R. (1997). Segregation of two spectrin isoforms: polarized membrane-binding sites direct polarized membrane skeleton assembly. *Mol. Biol. Cell* **8**, 1933-1942.

Edgar, L. G. (1995). Blastomere culture and analysis. In *Caenorhabditis elegans: Modern Biological Analysis of an Organism* (ed. H. F. Epstein and D. C. Shakes), pp. 303-320. Academic Press, San Diego.

Fire, A., Albertson, D., Harrison, S. W. and Moerman, D. G. (1991). Production of antisense RNA leads to effective and specific inhibition of gene expression in *C. elegans* muscle. *Development* **113**, 503-514.

Francis, R. and Waterston, R. H. (1991). Muscle cell attachment in *Caenorhabditis elegans*. *J. Cell Biol.* **114**, 465-479.

Gattung, S. and Wilson, R. K. (1996). The *C. elegans* cosmid K10B3. *EMBL/GenBank/DDBJ databases*, Accession number U49941.

Gattung, S., Pauley, A. and Wilson, R. (1996). The *C. elegans* cosmid K11C4. *EMBL/GenBank/DDBJ databases*, Accession number U64854.

Glenney, J. R., Glenney, P., Osborn, M. and Weber, K. (1982). An F-actin and calmodulin-binding protein from isolated intestinal brush borders has a morphology related to spectrin. *Cell* **28**, 843-854.

Guo, S. and Kemphues, K. (1995). *par-1*, a gene required for establishing polarity in *C. elegans* embryos, encodes a putative Ser/Thr kinase that is asymmetrically distributed. *Cell* **81**, 611-620.

Hodgkin, J. (1997). Appendix 1: Genetics. In *C. elegans II* (ed. D. L. Riddle, T. Blumenthal, B. Meyer and J. R. Preiss) pp. 881-1047. Cold Spring Harbor Laboratory Press, Plainview, New York.

Howe, C. L., Sacramone, L. M., Mooseker, M. S. and Morrow, J. S. (1985). Mechanisms of cytoskeletal regulation: modulation of membrane affinity in avian brush border and erythrocyte spectrins. *J. Cell Biol.* **101**, 1379-1385.

Kennedy, S. P., Warren, S. L., Forget, B. G. and Morrow, J. S. (1991). Ankyrin binds to the 15th repetitive unit of erythroid and nonerythroid β-spectrin. *J. Cell Biol.* **115**, 267-277.

Kenyon, C. (1986). A gene involved in the development of the posterior body region of *C. elegans*. *Cell* **46**, 477-487.

Kershaw, J. (1996). The *C. elegans* cosmid K12G11. *EMBL/GenBank/DDBJ databases*, Accession number Z81570.

Lee, J. K., Brandin, E., Branton, D. and Goldstein, L. S. B. (1997). α-spectrin is required for ovarian follicle monolayer integrity in *Drosophila melanogaster. Development* **124**, 353-362.

Lennard, N. (1997). The *C. elegans* cosmid R31. *EMBL/GenBank/DDBJ databases*, Accession number Z75956.

Miller, D. M., Stockdale, F. E. and Karn, J. (1986). Immunological identification of the genes encoding the four myosin heavy chain isoforms of *Caenorhabditis elegans*. *Proc. Nat. Acad. Sci. USA* **83**, 2305-2309.

Nelson, G. A., Lew, K. K. and Ward, S. (1978). Intersex, a temperature sensitive mutant of the nematode *Caenorhabditis elegans. Dev. Biol.* **66**, 386-409.

Patel, N. H. and Goodman, C. S. (1992). Preparation of digoxigenin-labeled single-stranded DNA probes. In *Non-radioactive Labeling and Detection of Biomolecules* (ed. C. Kessler), pp. 377-381. Springer-Verlag, Berlin.

Priess, J. R. and Hirsh, D. I. (1986). *Caenorhabditis elegans* morphogenesis: the role of the cytoskeleton in elongation of the embryo. *Dev. Biol.* **117**, 156-173.

Pulak, R. and Anderson, P. (1993). mRNA surveillance by the *Caenorhabditis elegans smg* genes. *Genes Dev.* **7**, 1885-1897.

Rhind, N. R., Miller, L. M., Kopczynski, J. B. and Meyer, B. J. (1995). *xol-1* acts as an early switch in the *C. elegans* male/hermaphrodite decision. *Cell* **8**, 71-82.

Rocheleau, C. E., Downs, W. D., Lin, R., Wittman, C., Bei, Y., Cha, Y. H., Ali, M. and Priess, J. R. (1997). Wnt signalling and an APC-related gene specify endoderm in early *C. elegans* embryos. *Cell* **90**, 707-716.

Seydoux, G. and Fire, A. (1994). Soma-germline asymmetry in the distributions of embryonic RNAs in *Caenorhabditis elegans*. *Development* **120**, 2823-2834.

Speicher, D. W., Desilva, T. M., Speicher, K. D., Ursitti, J. A., Hembrach, P. and Weglarz, L. (1993). Location of the human red cell spectrin tetramer binding site and detection of a related 'closed' hairpin loop dimer using proteolytic footprinting. *J. Biol. Chem.* **268**, 4227-4235.

Starich, T. A., Herman, R. K., Kari, C. K., Yeh, W.-H., Schackwitz, W. S., Schuyler, M. W., Collet, J., Thomas, J. H. and D. L. Riddle (1995). Mutations affecting the chemosensory neurons of *Caenorhabditis elegans*. *Genetics* **139**, 171-188.

Sulston, J. E. and Horvitz, H. R. (1977). Post-embryonic cell lineages of the nematode, *Caenorhabditis elegans*. *Dev. Biol.* **56**, 110-156.

Sulston, J. E., Schierenberg, E., White, J. G. and Thomson, J. N. (1983). The embryonic cell lineage of the nematode *Caenorhabditis elegans*. *Dev. Biol.* **100**, 64-119.

Thomas, G. H. and Kiehart, D. P. (1994). β_{Heavy}-spectrin has a restricted tissue and subcellular distribution during *Drosophila* embryogenesis. *Development* **120**, 2039-2050.

Thomas, G. H., Newbern, E. C., Korte, C. C., Bales, M. A., Muse, S. V., Clark, A. G. and Kiehart, D. P. (1997). Intragenic duplication and divergence in the spectrin superfamily of proteins. *Mol. Biol. Evol.* **14**, 1285-1295.

Thomas, G. H., Zarnescu, D. C., Juedes, A. E., Bales, M. A., Londergan, A., Korte, C. C. and Kiehart, D. P. (1998). Drosophila β_{Heavy}-spectrin is essential for development and contributes to specific cell fates in the eye. *Development* **125**, 2125-2134.

Waterston, R. and Sulston, J. (1995). The genome of *Caenorhabditis elegans*. *Proc. Nat. Acad. Sci. USA* **92**, 10836-10840.

Williams, B. D. and Waterston, R. H. (1994). Genes critical for muscle development and function in *Caenorhabditis elegans* identified through lethal mutations. *J. Cell Biol.* **124**, 475-490.

Williams-Masson, E. M., Malik, A. N. and Hardin, J. (1997). An actin-mediated two-step mechanism is required for ventral enclosure of the *C. elegans* hypodermis. *Development* **124**, 2889-2901.

Winkelmann, J. C. and Forget, B. G. (1993). Erythroid and nonerythroid spectrins. *Blood* **81**, 3173-3185.

Wissman, A., Ingles, J., McGhee, J. D. and Mains, P. (1997). *Caenorhabditis elegans* LET-502 is related to Rho-binding kinases and human myotonic dystrophy kinase and interacts genetically with a homolog of the regulatory subunit of smooth muscle myosin phosphatase to affect cell shape. *Genes Dev.* **11**, 409-422.

Yandell, M. D., Edgar, L. and Wood, W. B. (1994). Trimethylpsoralen induces small deletion mutations in *Caenorhabditis elegans*. *Proc. Nat. Acad. Sci. USA* **91**, 1381-1385.